AD-A095 136 NATIONAL BUREAU OF STANDARDS WASHINGTON DC SURFACE S--ETC F/G 7/4
THE USE OF ANGLE-RESOLVED ELECTRON AND PHOTON STIMULATED DESORP--ETC(U)
FEB 81 T E MADEY N00014-81-F-0021
UNCLASSIFIED TR-12 NL

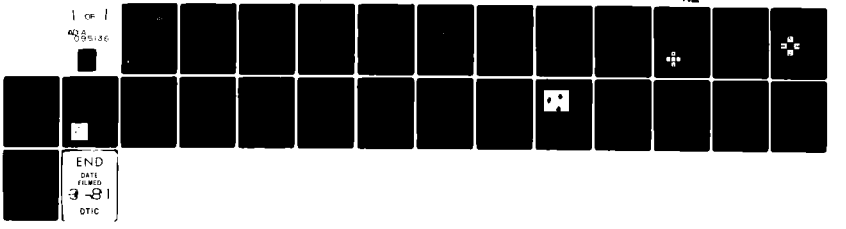

12

OFFICE OF NAVAL RESEARCH

Contract N00014-81-F-0021

LEVEL II

TECHNICAL REPORT NO. 12

THE USE OF ANGLE-RESOLVED ELECTRON AND PHOTON STIMULATED DESORPTION FOR SURFACE STRUCTURAL STUDIES

by

Theodore E. Madey
Surface Science Division
National Bureau of Standards
Washington, D. C. 20234

1 February 1981

To appear in Topics in Chemical Physics,
"Inelastic Ion-Surface Collisions",
Eds. W. Heiland and E. Taglauer
(Springer-Verlag, Heidelberg)

SECURITY CLASSIFICATION OF THIS PAGE (When Data Entered)

REPORT DOCUMENTATION PAGE		READ INSTRUCTIONS BEFORE COMPLETING FORM
1. REPORT NUMBER: Technical Report No. 12 ✓	2. GOVT ACCESSION NO.: AD-A095 736	3. RECIPIENT'S CATALOG NUMBER
4. TITLE (and Subtitle): (6) The Use of Angle-Resolved Electron and Photon Stimulated Desorption for Surface Structural Studies.		5. TYPE OF REPORT & PERIOD COVERED: ~~Interim~~
		6. PERFORMING ORG. REPORT NUMBER
7. AUTHOR(s): (10) Theodore E. Madey (12) 27		8. CONTRACT OR GRANT NUMBER(s): (15) N00014-81-F-0021
9. PERFORMING ORGANIZATION NAME AND ADDRESS: Surface Science Division ✓ National Bureau of Standards, Washington, DC 20234		10. PROGRAM ELEMENT, PROJECT, TASK AREA & WORK UNIT NUMBERS: (11) 2F-682
11. CONTROLLING OFFICE NAME AND ADDRESS: (14) Office of Naval Research Physical Program Office Arlington, VA 22217		12. REPORT DATE: February 1, 1981
		13. NUMBER OF PAGES
14. MONITORING AGENCY NAME & ADDRESS (if different from Controlling Office): (9) Technical Rept.		15. SECURITY CLASS. (of this report): Unclassified
		15a. DECLASSIFICATION/DOWNGRADING SCHEDULE

16. DISTRIBUTION STATEMENT (of this Report)

approved for Public Release; Distribution Unlimited

17. DISTRIBUTION STATEMENT (of the abstract entered in Block 20, if different from Report)

18. SUPPLEMENTARY NOTES

To be published in Topics in Chemical Physics

19. KEY WORDS (Continue on reverse side if necessary and identify by block number)

Surface, adsorption, desorption, electron stimulated desorption, surface structure, photon stimulated desorption, ion desorption

20. ABSTRACT (Continue on reverse side if necessary and identify by block number)

We review recent experiments and models related to desorption processes induced by electrons and photons incident on surfaces. The utility of angle-resolved electron and photon-stimulated desorption of ions for studies of molecular structure at surfaces is emphasized.

DD FORM 1 JAN 73 1473 EDITION OF 1 NOV 65 IS OBSOLETE
S/N 0102-014-6601 |

SECURITY CLASSIFICATION OF THIS PAGE (When Data Entered)

THE USE OF ANGLE-RESOLVED ELECTRON AND PHOTON STIMULATED DESORPTION FOR SURFACE STRUCTURAL STUDIES

Theodore E. Madey
Surface Science Division
National Bureau of Standards
Washington, D.C. 20234, USA

ABSTRACT

We review recent experiments and models related to desorption processes induced by electrons and photons incident on surfaces. The utility of angle-resolved electron and photon stimulated desorption of ions for studies of molecular structure at surfaces is emphasized.

I. Introduction

A continuing need in studies of atoms and molecules on surfaces concerns the location of surface bonding sites and the geometrical structure of molecules and molecular fragments on surfaces. That is, where are adsorbed species bonded, what are the directions of the bonding orbitals between the atom (molecule) and surface, and what are the bonding directions of ligands in adsorbed molecular complexes? In a continuing series of experiments [1,2], we have established that the electron stimulated desorption ion angular distribution (ESDIAD) method has clear potential for providing direct information regarding the site location and geometrical structure of molecules adsorbed on surfaces.

In this method, a surface containing adsorbed molecules is bombarded by a focused low energy electron beam. Electronic excitation of the adsorbed species by electron bombardment can result in the desorption of atomic and molecular ions from the surface [3-6]. The ions desorb in discrete cones of emission in directions determined by the orientation of the surface molecular bonds which are "broken" by the excitation. The resultant ESDIAD patterns provide a visual display of the geometrical structure of surface molecules in the adsorbed layer.

In the present paper, we shall review the experimental and theoretical developments concerning the relationship between ESDIAD and surface structure. Recent measurements of Photon Stimulated Desorption [7-9] (PSD) and angle-resolved PSD [10] of ions from surfaces using synchrotron radiation will also be discussed. It will be seen that in angle-resolved PSD [10], the potential exists to "tune" the incident radiation to determine the orientation of specific surface bonds.

The paper is organized as follows: Section II provides a general introduction to ESD phenomena, and Section III is a discussion of experimental procedures. The application of ESDIAD to various molecular systems is given in Section IV, along with a discussion of the role of steps and defects in ESD of oxygen monolayers. Section V is concerned with theoretical concepts regarding ESDIAD, and Section VI outlines the principles and recent results of angle-resolved PSD.

II. Basic Experimental Observations in Electron Stimulated Desorption

When a low energy electron beam bombards a surface containing an adsorbed monolayer, electronic excitation in the adsorbed layer may result in the desorption of ion or neutral fragments (including metastables) [3-6]. Thresholds for these excitations are typically in the range 10-50 eV, and the physical mechanisms for ion production are considered in detail by FEIBELMAN in this volume [11]. Electron bombardment can also cause dissociation and/or polymerization in surface layers. For electrons in the energy range 10 to 1000 eV incident upon metal surfaces containing an adsorbed monolayer of atoms or molecules, the general observations are as follows [1-6, 12]:

(a) Most ESD processes have cross sections which are smaller than those for electron-induced dissociation and ionization of gaseous molecules. For 100 eV electrons, typical gas phase dissociative ionization cross sections for small molecules are 10^{-16} cm^2. Typical cross sections for ESD of adsorbed molecules lie in the range 10^{-18} to 10^{-23} cm^2, with both lower and higher values observed for certain systems. Also, the cross sections for neutral desorption are generally larger than the cross sections for desorption of ions. Although ions frequently comprise a

small fraction of the desorbing species, the ease of experimental detection of ions means that their desorption characteristics are the most frequently studied ESD processes.

(b) Most ESD ions are atomic, with H^+, O^+, F^+ and Cl^+ being the most abundant. Negative ions of each of these four atoms have also been detected, [13, 14] but their yields are generally about 100 times smaller than for positive ions. The most common molecular ions reported from ESD of adsorbed monolayers are CO^+, OH^+, and OH^- [1-6]. ESD of multilayers can result in desorption of more complex molecular ions (i.e., $C_6H_{12}^+$ from a multilayer of C_6H_{12} [2], $H^+(H_2O)_n$ and $H^+(NH_3)_n$ from thick films of water and ammonia ice [15]).

(c) ESD cross sections are very sensitive to the mode of bonding. In general, cross sections for rupture of an internal bond in a weakly adsorbed molecule (the C...O bond in adsorbed CO, the H...C bond in adsorbed hydrocarbons, the H...O bond in adsorbed H_2O) are higher than cross sections for rupture of metal-atom bonds (low coverages of hydrogen or oxygen on a metal surface).

(d) The binding energies of chemisorbed molecules are sufficiently large that direct momentum transfer between electron and adsorbate does not provide sufficient energy to cause desorption of neutral species [5]. Power densities in most ESD studies are generally sufficiently low that thermal heating of the substrate does not induce desorption. These observations, coupled with the fact that ions are generally desorbed having most probable kinetic energies in the range 0 to 10 eV, indicates that ESD proceeds via an electronic excitation mechanism.

A one-dimensional FRANCK-CONDON excitation model of ESD has been developed independently by REDHEAD, and by MENZEL and GOMER [5], and is qualitatively consistent with the above observations. This model, along with the recent KNOTEK-FEIBELMAN Auger-Induced-Decay model of ESD have both been discussed extensively in the literature [1,3,6]. For a more extensive discussion of the mechanisms of ESD ion formation, the reader is referred to the paper by FEIBELMAN [11] in this volume.

The origin of angular effects in ESD will be discussed in V, and a summary of relevant experimental data relating ESDIAD to surface structure is discussed below.

III. Experimental Procedures

The ultrahigh vacuum apparatus used for most of the NBS ESDIAD studies has been described previously [1, 12] and is shown in Figure 1.

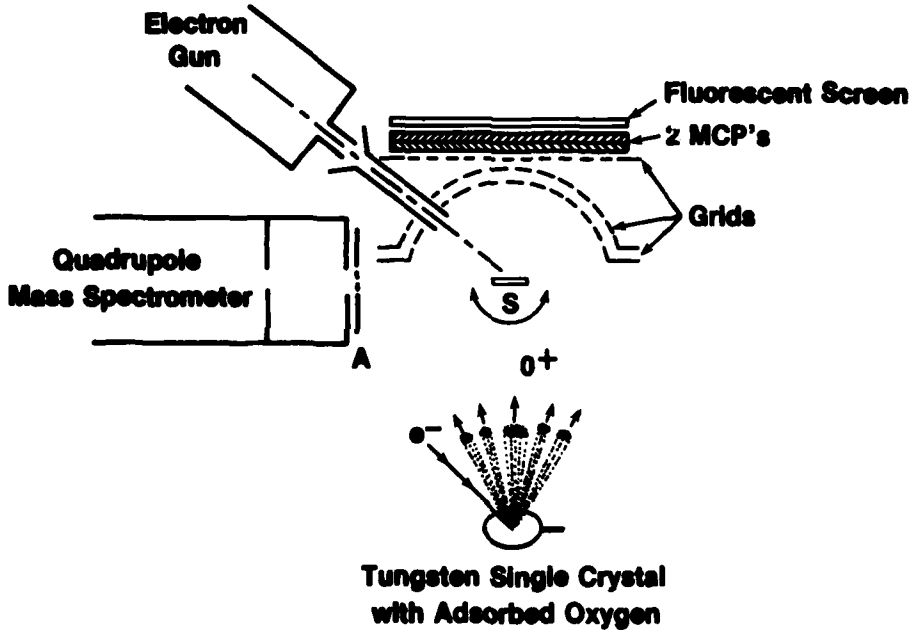

Figure 1. Schematic of ultrahigh vacuum ESDIAD apparatus. The sample S can be rotated about an axis normal to the plane of the drawing. ESD ions are mass analyzed in the quadrupole mass spectrometer, and ESDIAD patterns are displayed using the grid-microchannel plate (MCP) - fluorescent screen array. The lower drawing is a schematic of the ESDIAD process, in which O^+ ions are liberated in cones of emission during bombardment of the sample by a focused electron beam.

Briefly, a focused electron beam (50 to 1500 eV) bombards a crystal surface onto which gases have been deposited using a molecular beam doser. The ion beams which desorb from the crystal by electron stimulated desorption (ESD) pass through a hemispherical grid and are accelerated to a microchannel plate (MCP) assembly. The output signal from the MCP assembly is displayed visually on a fluorescent screen and photographed. By

reversing the potential of the input of the MCP assembly, the elastic low energy electron diffraction (LEED) pattern from the sample can also be studied. Mass identification of ESD ions are made using a quadrupole mass spectrometer (QMS). In addition, the QMS may be used as a detector in thermal desorption studies from the adsorbed layers. The cleanliness of the sample crystal is verified using Auger Electron Spectroscopy.

A schematic illustration of the ESDIAD process is shown at the bottom of Figure 1. A focused electron beam (e^-) bombards a single crystal containing a monolayer of adsorbed oxygen. The ESD O^+ ions are liberated in cones of emission, in specific directions related to the bonding geometry. The beams are intercepted by the MCP detector assembly, and displayed visually.

NIEHUS [16] has employed a channeltron multiplier as a moveable ion detector for measuring ESDIAD. His data are in the form of computer-generated plots of ion intensity as a function of ion desorption angle; he determines the mass of ESD ions using a Time of Flight method.

IV. Experimental ESDIAD Results

A. CO Adsorbed on Transition Metal Surfaces in Different Binding Configurations

Two examples [17,18] will be given (CO on Ru (001) and Pd (210)) where ESDIAD has been used to complement and verify structural information predicted using other methods, such as angular resolved ultraviolet photoemission spectroscopy, low energy electron diffraction, and surface vibrational spectroscopy [19]. In a third example, the adsorption of CO on stepped surfaces vicinal to W(110), entirely new insights into CO bonding configurations have been provided by this work [20].

As will be discussed in detail below, we have observed that when molecular CO is adsorbed on the close packed Ru(001) and W(110) surfaces, the dominant mode of bonding is via the carbon atom with the CO molecular axis perpendicular to the plane of the surface. For CO on atomically rough Pd(210) and for CO adsorbed at step sites on surfaces vicinal to

W(110), the axis of the molecule is tilted or inclined away from the normal.

a. CO on Ru(001)

Data previously reported using UPS (ultraviolet photoemission spectroscopy), EELS (electron energy loss spectroscopy), and reflection infrared spectroscopy have indicated that CO is terminally bonded to the Ru surface through the C atom, with the CO axis perpendicular to the surface. The ESDIAD results for CO confirm this orientation [17]: for all CO coverages in the temperature range 90K to 350K, the angular distributions of O^+ and CO^+ ESD ions are centered about the surface normal. The widths of the ion beams are temperature dependent; for both O^+ and CO^+, the corrected half widths at half maximum, α , of the ion cones are $\sim$ 14.5° at 300K and $\sim$ 11° at 90K. This temperature dependence, coupled with a simple model calculation, indicates that the dominant factors contributing to the width of ESD ion beams are initial state effects, i.e., CO surface bending vibrations of the type:

Since ion desorption times are short with respect to molecular vibration times, ESDIAD appears to sense the instantaneous statistical distribution of molecular orientations on the surface in this case. Thus, the data suggest that both the directions and widths of ESDIAD beams from adsorbed molecular species are determined largely by the structure and dynamics of the initial adsorbed state.

b. CO on Pd(210)

ESDIAD has been used to verify an unusual bonding configuration for CO on the (210) surface of fcc palladium [18]. In an infrared reflection-adsorption study [19] of CO on Pd(210) and (100), the measured values of the C-O stretching frequency indicated that at low coverage, the CO is bridge-bonded to two Pd atoms via the C atom. The Pd(210) is a rather open surface, and top layer atoms with the nearest neighbor distance of

2.73 Å do not exist (see Fig. 2); the shortest distance between top layer atoms is 3.88 Å in the [001] direction. Bridge-bonding is not known to occur in transition metal carbonyls for metal-metal spacings greater than ∿ 2.78 Å. On Pd(210), it therefore appears that bridge-bonding can only occur on sites of the kind which exist between atoms in the first and second atom layers, so that the axes of adsorbed CO molecules are expected to be inclined away from the normal by ∿ 18° as shown for the type C site in Figure 2.

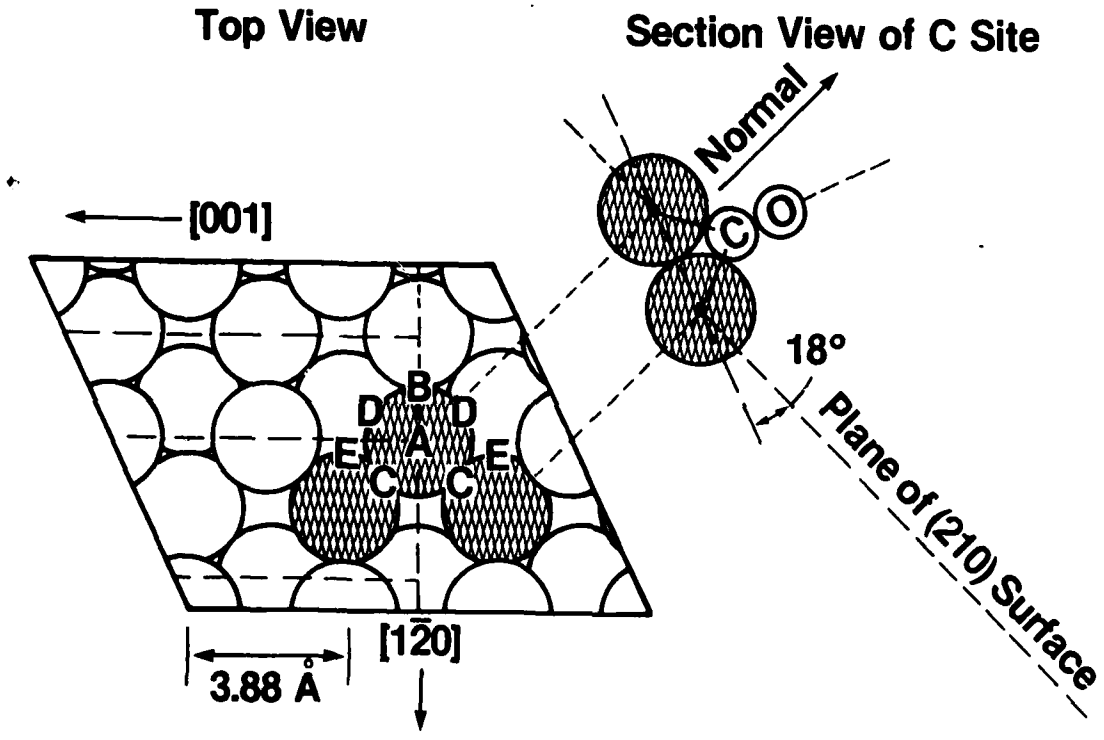

Figure 2. Model of Pd(210) surface with possible bonding sites for CO labeled. The section view illustrates how the CO molecule is "inclined" in the C sites (from Ref. 18, with permission).

The ESDIAD data are consistent with the infrared results, and for CO coverages θ less than 0.5 monolayers, two-fold symmetric ion desorption patterns dominated by emission in directions away from the normal are observed. In addition, the ESDIAD patterns provide specific information about the desorption sites. CO populates the two equivalent type C sites at $\theta < 0.5$, and type B sites at higher coverages. Furthermore, the ESDIAD results indicate that the surface bending vibrational amplitudes for the bridge-bonded CO are different in orthogonal directions, in agreement with recent calculations [21]. At the saturation CO coverage ($\theta = 1$) at 90K, at

least a fraction of the adsorbed CO appears to be bonded with the molecular axis normal to the Pd(210) surface.

c. CO on W(110) and Stepped Surfaces Vicinal to W(110)

The above results demonstrate that the ESDIAD method yields CO structures consistent with adsorbed molecular geometries deduced using other techniques. Based on these data, we have examined the role of surface steps in molecular adsorption in an ESDIAD study of CO on a multifaceted tungsten monocrystal [20]. The questions to be answered are: How do the CO adsorption geometries compare on flat surfaces and on stepped surfaces, and are new structures seen on stepped surfaces? The experiments were performed on a 7mm diam. tungsten crystal cut to expose 5 separate facets. It was also used in an ESDIAD study of oxygen adsorption [22] which will be discussed in IV.B., and was similar to one used in studies of oxygen adsorption kinetics on stepped surfaces [23]. The central facet was oriented within 0.3° of the (110) plane, and the four surrounding facets were stepped surfaces of different step densities (6° and 10° off the (110) plane), and with step orientations parallel to [100] and [110] directions. The ESDIAD patterns seen for a monolayer of CO adsorbed on this multifaceted sample at 273K are shown in Figure 3.

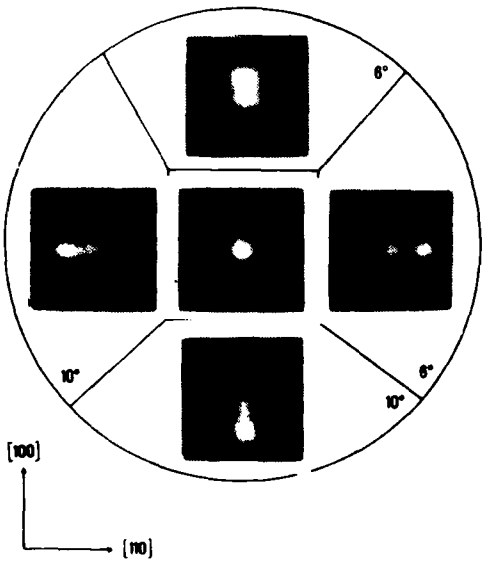

Figure 3. ESDIAD patterns for desorption of ions from CO adsorbed at 273K on the multifaceted W crystal described in the text. The central facet is oriented with its surface parallel to the (110) plane and the (110) terrace widths on the 6° and 10° stepped surfaces are 13Å and 22Å respectively. In all of the patterns, the spot in the center of the picture corresponds to a beam of O^+ and CO^+ ions desorbing normal to the surface. The off-normal beams from each of the faceted surfaces provide evidence for "inclined" CO. (From Ref. 20, with permission).

The electron beam was scanned from facet to facet, and the patterns were photographed from the fluorescent screen. The central W(110) facet yields a single ESDIAD beam which desorbs perpendicular to the surface, giving a single spot in the center of the photograph. Each of the stepped surfaces also yields an ESD ion beam which desorbs perpendicular to the (110) terraces; the images of these normal beams appear in the center of the photos for each of the 4 outer facets in Figure 3. In addition, each stepped facet yields an extra ESD ion beam which desorbs in a down-step direction, along an azimuth perpendicular to the step edge. All beams consist of both O^+ and CO^+, in approximately equal intensities. The polar angle between the normal and off-normal beams on the right and left facets is $\sim 40°$.

We interpret these data as follows: At 273K, CO adsorbs in molecular form (the virgin state) along with some dissociated CO (the β states) [24]. The ESD signal is due primarily to the molecular CO. Ultraviolet photoemission data demonstrate that molecular virgin CO is bonded to tungsten through the carbon atom [25]. The single normal beam seen in the ESDIAD pattern for CO on W(110) indicates that the molecular CO is bonded perpendicular to the W(110) facet. On each of the stepped surfaces, a fraction of the molecular CO is also bonded with the molecular axis perpendicular to the W(110) terraces. In addition, the observation of the down-step ion beams indicates that the CO molecules are tilted away from the normal to the terraces by $\sim$ 40°, and are probably adsorbed directly on the edges of the steps. A preliminary account of the temperature dependence of CO bonding configurations on the multifaceted W crystal has been published elsewhere [20].

Finally, we note that JAEGER and MENZEL [26] have also found evidence for "inclined" CO in an ESDIAD study of CO on W(100). They conclude that the CO is bound on different sites, including both symmetric and asymmetric bridges.

B. The Role of Steps in ESD of Adsorbed Atoms: Oxygen on Tungsten

In a large number of studies of oxygen on tungsten using ESD [27], it has been found that there is little or no O^+ ion yield at low oxygen coverages. Only where the surface coverage is greater than 0.5 to 0.75 monolayers is

significant O^+ ion signal seen. Several models of this "induction period" in the appearance of O^+ during oxygen adsorption have been offered, including local oxide formation, the adsorption of a new molecular state, and bonding at special sites on the surface [27]. In order to systematically investigate to what extent sites such as atomic steps and defects might influence the ESD of O^+ from adsorbed oxygen, we have studied the adsorption of oxygen [22] on the same polyhedral W crystal discussed in IV. A.c. Upon adsorption at 300K, there is little or no ESD O^+ emission from the flat W(110) plane at any oxygen coverage. In contrast, adsorption of oxygen on stepped surfaces vicinal to W(110) yields intense O^+ emission normal to the terraces and in "downstep" directions, as seen using ESDIAD and shown in Figure 4.

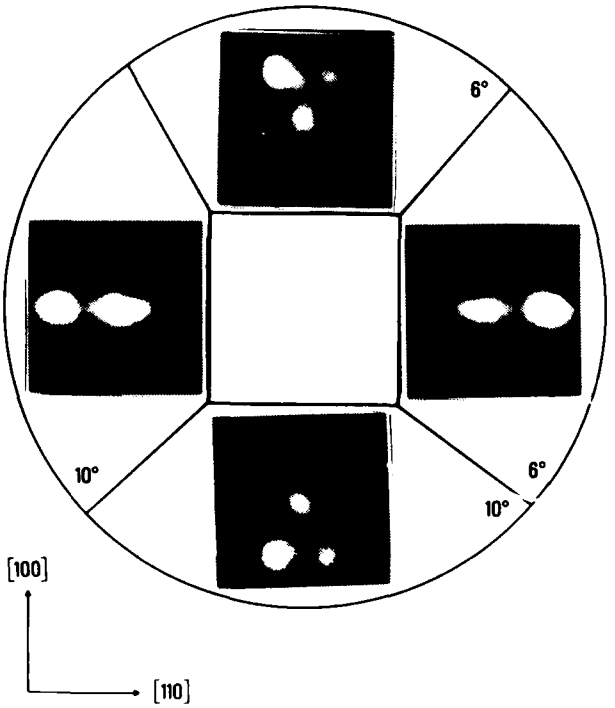

Figure 4. ESDIAD patterns for adsorption of oxygen on multifaceted tungsten crystal described in the text. $T_{ads} \simeq$ 300K. The center of each pattern corresponds to the normal to the (110) terrace. The outer beams are due to ESD of O^+ in directions away from the normal. See Fig. 3 for more details. (From Ref. 22, with permission).

The data suggest that the "ESD-active" sites for O^+ desorption from oxygen on tungsten are low coordination sites which are absent on a perfect W(110) surface, but present on the stepped surface. It appears that the adsorption of oxygen atop substrate atoms at step edges is necessary for the ESD of O^+ from W surfaces containing (110) terraces; oxygen adsorbed on the (110) terraces does not yield a significant ESD ion signal. In contrast, oxygen adsorbed on the more open W(100) surface does yield an appreciable O^+ signal;

even for this surface, however, adsorption at step sites leads to enhanced O^+ desorption [28].

Two possible explanations can be offered to explain this sensitivity of ESD to atomic adsorption at low coordination sites. First of all, on the basis of the one dimensional REDHEAD-MENZEL-GOMER [5] model of ESD, the probability of ionic desorption P_I is exponentially related to the neutralization rate for an ion formed at the surface by electron bombardment, viz.,

$$P_I = \exp-\left\{ \int_{x_0}^{\infty} \frac{R(x)}{v(x)} \, dx \right\}$$

where R(x) is the neutralization rate (sec^{-1}), v(x) is the ionic velocity in the repulsive final state, x is the distance from the surface, and x_0 is the separation between atom and surface at the point of excitation. R(x) is a measure of the rate of electron transfer (i.e., tunneling, Auger neutralization) from the substrate to the ion created by electron bombardment, and it is reasonable to assume that R(x) is different for adatoms bonded in different sites. Oxygen atoms adsorbed on W(110) flats are located in multiply-coordinated sites, bonded to 2 or 3 substrate W atoms [29]; oxygen atoms adsorbed at step edges may be in atop sites, bonded to single W atoms. An increase in coordination (i.e., the "number of bonds" to the substrate) should result in an increase in R(x) and a corresponding decrease in P_I at that site. Since P_I is exponentially dependent on R(x), even small changes in R(x) will have a strong influence on the ESD ion desorption probability P_I.

In accordance with the KNOTEK-FEIBELMAN [6] model of ion desorption, another interpretation of the enhanced O^+ emission from step edges may involve the formation of oxide-like complexes at step sites, with the enhanced yield due to the Auger decay mechanism. Careful measurements of the thresholds for ion desorption are not available for stepped W(110) surfaces, but O^+ desorption thresholds measured in recent PSD studies of oxygen on W(111) [10] and W(100) [9] indicate that the O^+ signal may indeed originate from oxide-like species on these surfaces. These data will be discussed in Section VI.

Thus, both for non-dissociative adsorption (in which mainly internal molecular bonds are ruptured by ESD, i.e., O^+ from CO/W) and for dissociative adsorption (in which metal-adsorbate bonds are ruptured by ESD, i.e., O^+ from O/W), the ESDIAD structures are sensitive to the presence of steps and defects on metal surfaces. The widespread occurrence of "off-normal" ESDIAD beams from stepped surfaces indicates that there are many instances of "inclined" molecular structures on surfaces. Finally, the ESD ion yield is rather high from molecular adsorbates (i.e., CO) on planar W(110) surface but very low for atomic oxygen.

C. Application of ESDIAD to Other Molecular Adsorbates.

ESDIAD has been applied to a number of molecular systems in addition to those already discussed. Particularly interesting observations have been made in the cases of H_2O and NH_3 on Ru(001) [2,30] and NH_3 on Ni(111) [31]; for low coverages of these adsorbates, the characteristic ESDIAD pattern in all 3 cases has the appearance of a "halo", i.e., a continuous band of emission on an off-normal direction with little emission normal to the surface. An example is shown in Fig. 5, corresponding to ~ 0.5 monolayers of NH_3 on Ni(111) at 160K. The structures suggested by the halo patterns are arrays of species such as

Figure 5. ESDIAD pattern for ESD of NH_3 on Ni(111); $\theta<1$, $T_{ads} \gtrsim 160K$. Total electron energy was 350 eV: a bias potential of 200 V was applied to the sample to "compress" the ion pattern.

Such structures are also consistent with UPS evidence, as well as with an EELS study of H_2O on Ru(001) [32]. Evidence for rotational (azimuthal) ordering at higher coverages ($\theta > 0.5$) was seen for H_2O and NH_3 on Ru(001), but not for NH_3 on Ni(111).

A fractional monolayer of C_6H_{12} adsorbed on Ru(001) yields a hexagonal H^+ ESDIAD pattern [2]. These results indicate the azimuthal orientation of the C-H bonds, and are consistent with a simple model of C_6H_{12} adsorption. The C_6H_{12} appears to be adsorbed directly over Ru substrate atoms in a "tilted chair" configuration. These data for H_2O, NH_3 and C_6H_{12} indicate several of the advantages of ESDIAD in determining the structure of molecules at surfaces, namely:

- ESDIAD reveals structures consistent with the molecular geometry predicted using other methods
- ESDIAD is particularly sensitive to the azimuthal orientation of hydrogen ligands in adsorbed molecules. In general, electron scattering from H in molecules is too weak to allow LEED to be useful.
- ESDIAD is sensitive to the <u>local</u> bonding geometry. It is not a diffraction method, so long range surface order is not necessary to produce a sharp ESDIAD pattern.

V. Origin of Angular Effects in ESD

Since the first experimental observations of the ESDIAD phenomenon, there have been only a few articles which have specifically addressed the theory of ion angular distribution in ESD. GERSTEN, JANOW and TZOAR [33] were the first to use dynamical arguments to link the observed angular distribution patterns to details of the bonding of adatoms on surfaces. They reported model calculations of angular distributions of O^+ ions desorbing from oxygen adsorbed at different sites on model W(100) and W(111) surfaces. A MAXWELL-BOLTZMANN distribution was used to approximate the distribution of atom positions about each site due to vibrations. The atoms were converted to ions by the excitation process, and the positive ion-

solid potential was modeled assuming atomic wave functions and an unrelaxed lattice. Asymptotic ion trajectories were computed classically and plotted graphically. Details of the patterns were found to vary sensitively with changes in surface bonding geometry. Beams desorbing in off-normal directions were invariably due to oxygen atoms located in non-high-symmetry sites; beams desorbing normal to the surface were due to oxygen bonded in sites atop substrate atoms.

CLINTON [34] has formulated a quantum scattering theory of ESD in which he assumes that the final state potential experienced by the ion following excitation is a sum of central potentials. In this model, the initial direction of ion desorption occurs along a chemical bond direction (ignoring anisotropies in reneutralization). Thus, he concludes that ESDIAD processes are dominated by the initial state (ground state) structures of atoms and molecules on surfaces. He also suggests that the widths of ion beams are due, in large part, to bending vibrations of the adsorbed species.

In the KNOTEK-FEIBELMAN Auger-induced-decay model [6], ion desorption from maximal valency transition metal oxides involves COULOMB repulsion between a multiply charged cation (W^{6+} in WO_3, Ti^{4+} in TiO_2, etc.) and an anion which has acquired a positive charge (e.g., O^+) due to an interatomic Auger transition. Since the dominant force is the Coulomb repulsion along the line of centers between cation and anion, the initial impulse experienced by the desorbing ion (O^+, in this case) will be directly determined by the original bond direction. Of course, a complete description of the desorbing ion's trajectory requires a knowledge of the electrostatic potential outside the surface of the ionic crystal.

A consideration of the timescales in ESD also leads to the conclusion that in most cases, the initial ion desorption direction should be related to the initial state bond angle. Molecular vibration and rotation times are 10^{-12} to 10^{-13} sec, much slower than typical ion desorption times (10^{-14} to 10^{-15} s). For example, an H^+ ion desorbing with 2 eV kinetic energy will travel 1Å in 5×10^{-15}s, and an 8 eV O^+ ion will travel 1Å in 1×10^{-14}s. After an ion has moved $\sim$ 1Å from the equilibrium bond distance, the probability of recapture by neutralization is small. Ion desorption

times are sufficiently rapid with respect to vibration times that significant molecular rearrangements are unlikely to occur prior to desorption. Thus the ion desorption angle should be related to the initial bond angle.

Now, we consider to what extent final state effects perturb the ion trajectories. Several final state factors which have been suggested previously [17,26] include: anisotropy in the reneutralization rate (structure in the imaginary part of the final state potential), "defocussing" due to structure or curvature in the real part of the final state potential, and deflection of the ion trajectory due to the image force acting on the desorbing ion. In the absence of detailed knowledge of the final state potentials, we have no basis for estimating the first two factors. We can, however, estimate the influence of the image potential. CLINTON [34] has shown that an ion desorbing with an initial angle α_i with respect to the surface normal will arrive at the detector with an apparent desorption angle α_o given by

$$\cos \alpha_o = \cos \alpha_i \left[\frac{1 + V_I/[(E_K-V_I) \cos^2 \alpha_i]}{1+V_I/(E_K-V_I)} \right]^{1/2} \qquad (1)$$

Here, V_I is the (screened) image potential at the initial ion-surface separation Z_o [35a] (using Gadzuk's procedure [35b] to locate the image plane), and E_K is the final (measured) kinetic energy of the desorbed ion. Note that V_I is a negative quantity so that $\left|V_I/(E_K-V_I)\right|$ is ≤ 1 and $\alpha_o > \alpha_i$. The straightforward derivation of eq. (1) assumes a step-like "hard wall" repulsive final state potential.

From eq. (1), it is clear that the image potential acts to systematically increase the measured desorption angle α_o over the initial desorption angle α_i <u>in all cases</u>. The magnitude of the correction is greater for large values of α, and low values of E_K, and vice versa. For example, if we insert in eq. (1) values appropriate to the desorption of O^+ from CO on Ru(001) (V_I = 1.52 eV, E_K = 7 eV, Z_o = 1.9 Å) eq. (1) predicts that α_i = 14.5° when α_o = 16° and α_i = 10.8° when α_o = 12°, corrections of the order of 10% in the polar desorption angle. A much larger effect is seen for lower energy ions desorbing with a large value of α_i. For V_I=-2.62 eV,

E_K=4 eV, and Z_o=1.04 Å (appropriate to a "bent" NH species adsorbed on Ni(111)), α_o = 80° when α_i = 50°, a substantial correction.

Implicit also in eq. (1) is the existence of a cut-off angle for ion desorption. Specifically, for

$$\frac{V_I}{(E_K - V_I)\cos^2\alpha_i} > 1 \qquad (2)$$

there will be no escape of the desorbing ion. For values of α_i slightly greater than the cut-off value, the ions will follow shallow trajectories and strike the surface at some distance from the point of excitation. An interesting consequence may be that the bombardment of surface molecules by low energy ESD ions following shallow trajectories can induce chemical changes in the adlayer!

Thus, the image potential can have a major influence on the polar component of the ion desorption angle. The question now arises: What about the azimuthal component of the ion desorption angle, i.e., the desorption angle projected into the plane of the surface? For desorption from a perfectly plane surface, or along an azimuth of symmetry, there are no "torques" expected to influence the azimuthal angle. For desorption from a site of lower symmetry, azimuthal anisotropy in either the final state repulsive potential or the reneutralization probability could cause deviation of the ion trajectories in the azimuthal direction. From an experimental point of view, the frequent occurrence of ESDIAD beams having nearly circular cross sections suggests that azimuthal deflections of the desorbing ions are not a general problem.

It thus appears that, in general, the directions of ion desorption are determined largely by the structure of the adsorbed complex in its ground (initial) state. The only consistently predictable perturbation of the ion trajectories is due to the image potential; this invariably results in a deflection of the polar angle to larger values. There do not appear to be systematic effects which influence the azimuthal component of the ion desorption angle.

Finally, we note that measurements of the angular distributions of neutral species released in ESD would be useful in avoiding those electrostatic effects which perturb the trajectories of ions. Desorption angles in neutral ESD should bear a much more direct relation to bond angles than in ESDIAD! These (difficult) experiments are being planned in several laboratories.

VI. Photon Stimulated Desorption

A. Angle-Resolved PSD Using Synchrotron Radiation

For a number of years, it was thought that the photon stimulated desorption (PSD) of species from surfaces was a relatively inefficient and unimportant process [36]. A new impetus was given to PSD studies when KNOTEK and FEIBELMAN [6,11] proposed their core hole Auger decay mechanism, which predicts that ion desorption from ionically bonded species at surfaces is initiated by the formation of shallow core holes in surface atoms. An essential feature of the model is that ion desorption occurs independent of the manner of production of the core hole, whether it is excited by electrons or photons. The first demonstration of PSD of ions via core hole excitation using synchrotron radiation was made by KNOTEK, JONES and REHN [7], who observed ion desorption from adsorbed species on TiO_2. The PSD of ions from a metal surface (O^+ from oxygen on W(100)) was observed by WOODRUFF, TRAUM et. al. [9], who also showed the essential equivalence between ESD and PSD threshold energies. The PSD of ions by X-Ray photons was seen by FRANCHY and MENZEL [8], and will be discussed in VI (B) below.

To date, there are only two clearcut examples of the use of Angle-Resolved PSD for studying surface geometrical structures: VAN DER VEEN et. al. [37] measured the energy and angular distributions of PSD ions from a cleaved V_2O_5-(010) surface and MADEY et. al. [10] have measured ion angular distributions for O^+ desorption from a W(111) crystal, as well as photon excitation spectra for O^+ ion desorption. In both cases, good agreement was found with ESDIAD results for the same systems. However, as shall be seen below, the sharpness of the PSD threshold energies indicate that angle resolved PSD has clear potential for determining the bonding structures of adsorbed atoms and molecules, by selective excitation of sur-

face species having different energy thresholds for ion desorption.

Using a unique display-type analyzer, VAN DER VEEN et. al. [37] studied the PSD of O^+ from a V_2O_5(010) surface. The ellipsoidal mirror analyzer with a microchannel plate detector array was designed by EASTMAN et. al. [38] primarily for angle-resolved UPS studies, and was adapted specifically for this study. In addition to determining ion energy distributions, the authors were able to mass-analyze the desorbing ions using time-of-flight gating techniques. The angular distribution of desorbed O^+ ions was found to be strongly peaked in the direction of the surface normal. The strongly directional desorption pattern reflects the local bonding geometry of the initial state surface oxygen atoms, and is consistent with a previously proposed structural model of the V_2O_5 (010) surface [39]. In this model, the outermost surface oxygen atoms ($\sim 5 \times 10^{14}$ atoms/cm^2) occupy sites directly atop vanadium atoms, with a bond direction parallel to the surface normal. The observed photoexcitation spectrum of the O^+ ion yield was seen to be consistent with the core hole Auger decay model [6,11], and showed convincingly that the desorbed oxygen had been originally bonded to substrate V atoms. Thus, both the bonding site and the surface bond angle were identified experimentally.

In a search for strong angular anisotropies in PSD from a well-characterized monolayer adsorbed on a metal surface, a joint NBS-IBM group [10] used the EASTMAN [38] analyzer to study oxygen adsorbed on a W(111) surface. The primary objective was to determine whether or not the angular distribution of O^+ ions observed in ESDIAD [40, 41], i.e., discrete off-normal O^+ beams, would also be seen in PSD ion angular distributions.

Figure 6 is a PSD angular distribution pattern for an oxidized W(111) surface [10], and corresponds to O^+ ion desorption excited by photons of energy $h\nu$ = 45eV. The three O^+ beams are symmetrically disposed about the surface normal, each having a polar angle α of 41 $\pm$ 2° with respect to the normal. The value of α depends on coverage and temperature, and is 27° $\pm$ 3° in the similar PSD pattern observed for monolayer oxygen at 300K. These experiments indicate that the symmetry, azimuthal orientation and angular separations of the PSD patterns are identical to those of the ESDIAD patterns excited by 500 eV electrons as well as those reported previously [40, 41].

Figure 7 is taken from Ref. [10], and contains plots of the O^+ ion yield, corrected for photon flux, as a function of photon energy. Fig. 7b corresponds to the oxide surface ($\gtrsim$ 3 monolayers of oxide) 7c is the yield from an oxygen monolayer and 7d is the yield from $\sim$ 0.5 monolayer of oxygen. For each of these curves, the ions were determined to be O^+ using a time-of-flight method. The distinct "breaks" or onsets in the yield curves correspond roughly to the core-hole binding energies for tungsten atoms in solid W and WO_3 [42] indicated on the figure. We note that curve 7c is similar to PSD data for an oxygen monolayer on W(100) [9]. Of particular interest is the similarity between the ion yield curves and the secondary electron yield curve of Fig. 7a measured for the surface with the monolayer of oxygen. Such a constant-final state ($\sim$ 3 eV kinetic energy electrons) plot of the secondary electron cascade has been shown to be directly proportional to the soft x-ray absorption coefficient. Although most of the structure in Fig. 7a is due to such inelastic processes, the sharp peaks at 40 and 43 eV are due to direct emission via W 4f levels.

The overall agreement between ion yields and secondary electron yields indicates that photo-induced excitations of substrate W atoms plays a major role in the desorption of ions, consistent with the KNOTEK-FEIBELMAN model. The differences in detail are likely due to the fact that PSD ions originate only from the top layer of surface atoms for which the local density of states is different from that in the bulk, whereas the secondary yield curve results largely from pure W metal.

All three of the ion yield curves in Fig. 7 are dominated by peaks at 45 and 55 eV. This suggests that the O^+ - yielding species for $\theta < 1$, $\theta \sim 1$ and the oxide layer have similar electronic configurations. The simplest formulation of the Auger decay model of ion desorption requires maximal valency for the cationic species (e.g., W^{6+} as in WO_3); reduced forms of the oxide result in little or no PSD ion yield due to the increased valence electron density on the cation, as in W^{4+}. The data thus indicate that maximal valency species are present even in monolayers and fractional monolayers of oxygen. Such species could be WO_3 - like molecular species, or they could be oxygen atoms bonded to special sites (steps, defects) at which the valence charge density on the W is lowered

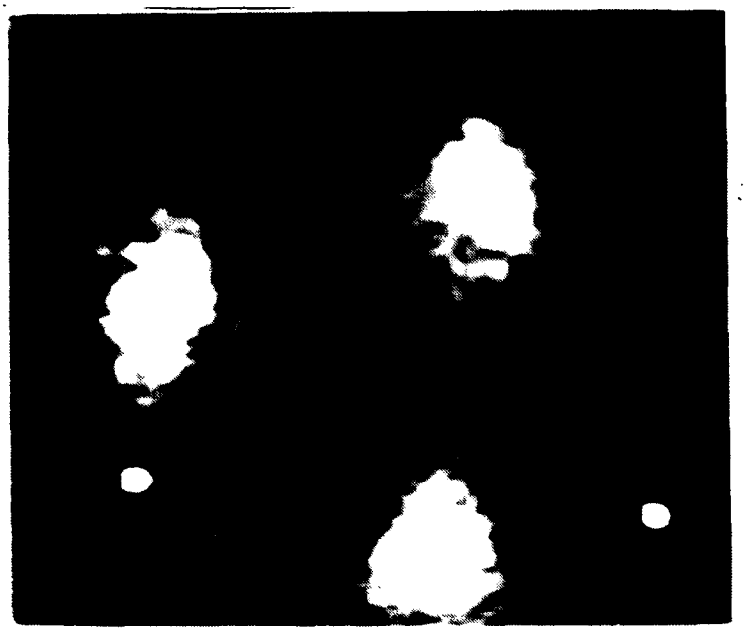

Figure 6. PSD ion angular distribution patterns for O^+ desorption from the oxidized W(111) surface for a photon energy of 35.4 eV. The two small white dots are markers on the detector screen (From Ref. 10, with permission).

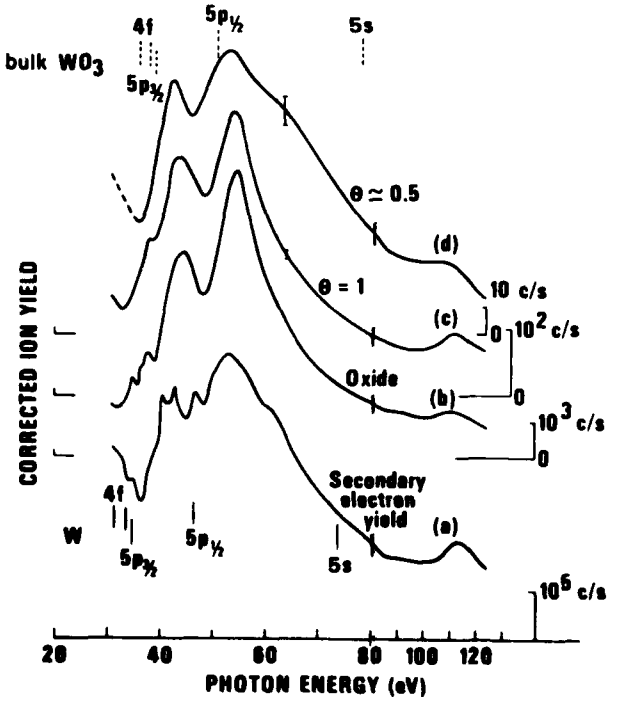

Figure 7. Electron and ion yields for W(111) as a function of photon energy, corrected for monochromator transmission and second-order contributions. Ion Yields are normalized to the same incident flux. Curve a, secondary electron yield at constant final state (E_{kin} = 3eV) for an oxygen monolayer. Curve b, O^+ ion yield from an oxide layer. Curve c, O^+ yield from an oxygen monolayer. Curve d, O^+ yield from an 0.5 monolayer coverage. Binding energies for W core levels in pure W (solid lines) and WO_3 (dashed lines) are shown. The energy scale changes at 80 eV (From Ref. 10, with permission).

due to its reduced coordination to the substrate. As indicated by the relative intensities of curves b-d in Fig. 7, such species must have a low concentration at coverages < 1 monolayer, and hence ESD and PSD of O^+ from W is due to a "minority species." As discussed in Section IV B and Ref. [22], the O^+ yielding sites on stepped surfaces vicinal to W(110) were shown to be minority sites, i.e., steps and defects.

The question logically arises: since angle resolved PSD requires a synchrotron, isn't it easier to use ESDIAD for characterizing the structures of molecules at surfaces? In many cases, the answer is yes. However, the sharp thresholds for PSD of ions (in contrast to the rather broad excitation spectra seen in electron bombardment, due to inelastic effects) [6] means that selective excitation and desorption of specific adsorbed atoms or molecules is possible. In a complex overlayer, PSD using a tuneable source offers the promise of selective desorption and structural determination of specific adsorbed species bonded to single substrate elements. In addition, the ion current above a core hole threshold is proportional to the core ionization cross section; its energy dependence in PSD will exhibit extended x-ray absorption fine structure (EXAFS) [7, 8, 43]. If the PSD ion current is used as an EXAFS monitor, the distance between an adsorbate atom and its neighbors can be determined, in principle.

B. Deep Core Excitations by Electrons and Photons

FRANCHY and MENZEL [8] have shown that soft-X-ray induced ion desorption from a covalently bound adsorption layer on a metal surface (CO on W(100)) is caused by an intrinsic photoprocess identified as adsorbate core hole ionization, followed by Auger decay. This process is the surface analog of gas phase molecular decomposition processes following deep core ionization [44]. They further demonstrated a substantial enhancement of the electron stimulated desorption cross sections for CO^+ and O^+ desorption at primary energies greater than the C1s and O1s core hole ionization energies, respectively. HOUSTON and MADEY [45] have also found that the cross section for O^+ desorption for virgin CO on W(110) increases sharply for electron energies greater than the O1s binding energy; very recently, similar observations were made for CO and NO on Ni(111) [46].

The first explanation of desorption processes initiated by adsorbate core ionization [8] is the effect known as "Coulombic Explosion" in molecules [44]: Auger decay, including Auger cascades, of the primary core hole results in accumulation of positive charge on the originally core-ionized atom and its bonded neighbors, which fly apart by Coulomb repulsion. It has been recently suggested [47-49] that the desorption mechanism hinges on final state hole localization (such as two holes in the 1π bonding orbital of molecular CO) which can lead to destabilization of bonding, and dissociative ionization. The effect of multiple electron excitations in ESD and PSD of molecular adsorbates is an active area of experimental [50] and theoretical [47-49] interest and we are on the threshold of new insights into the mechanisms of these important processes.

VI. Epilogue

Angle Resolved ESD and PSD studies are providing direct and useful insights into the geometrical and electronic properties of surfaces with adsorbed layers. It is clear that these two tools are unique additions to the ever-growing arsenal of methods for probing surfaces.

VII. Acknowledgements

The author acknowledges with pleasure a host of collaborators who have contributed substantially to the research and ideas discussed herein: J. T. Yates, Jr. and R. Stockbauer (NBS), J. E. Houston (Sandia), S. C. Dahlberg (Bell), J. F. van der Veen and D. E. Eastman (IBM), A. M. Bradshaw and F. M. Hoffmann (Fritz Haber Inst.) and C. Seabury and T. N. Rhodin, (Cornell). Valuable conversations were held with D. Menzel, P. Feibelman, and W. L. Clinton. This work was supported in part by the U. S. Office of Naval Research.

REFERENCES

1) T. E. Madey and J. T. Yates, Jr., Surface Sci. 63, 203 (1977).

2) T. E. Madey and J. T. Yates, Jr., Chem. Phys. Letters 51, 77 (1977); Surface Science 76, 397 (1978).

3) D. Menzel, in Interactions on Metal Surfaces, ed. R. Gomer, Topics Appl. Phys. vol. 4, (Springer, Heidelberg, 1975) p. 101; and Surface Sci. 47, 370 (1975).

4) T. E. Madey and J. T. Yates, Jr., J. Vac. Sci. Technol. 8, 525 (1971).

5) D. Menzel and R. Gomer, J. Chem. Phys. 41, 3311 (1964); P. A. Redhead, Can. J. Phys. 42, 886 (1964).

6) M. L. Knotek and P. J. Feibelman, Phys. Rev. Lett. 40, 964 (1978); P. J. Feibelman and M. L. Knotek, Phys. Rev. B 18, 6531 (1978).

7) M. L. Knotek, V. O. Jones, and V. Rehn, Phys. Rev. Lett. 43, 300 (1979).

8) R. Franchy and D. Menzel, Phys. Rev. Lett. 43, 865 (1979).

9) D. P. Woodruff, M. M. Traum, H. H. Farrell, N. V. Smith, P. D. Johnson, D. A. King, R. L. Benbow, and Z. Hurych, Phys. Rev. B 21, 5642 (1980).

10) T. E. Madey, R. L. Stockbauer, J. F. van der Veen and D. E. Eastman, Phys. Rev. Lett. 45, 187 (1980).

11) P. J. Feibelman, this volume.

12) T. E. Madey, in Methods of Experimental Physics, Vol. , "Methods of Experimental Surface Science," R. L. Park, ed., (Academic Press, N.Y.) to be published.

13) A. Kh. Ayukhanov and E. Turmashev, Soviet Physics - Tech. Phys. 22, 1289 (1977); J. L. Hock and D. Lichtman, Surface Sci. 77, L184 (1978).

14) M. L. Yu, Surface Sci. 84, L493 (1979).

15) R. H. Prince and G. R. Floyd, Chem. Phys. Lett. 43, 326 (1976).

16) H. Niehus, Surface Sci. 78, 667 (1978); Surface Sci. 80, 245 (1979).

17) T. E. Madey, Surface Science 79, 575 (1979).

18) T. E. Madey, J. T. Yates, Jr., A. M. Bradshaw, and F. M. Hoffmann, Surface Sci. 89, 370 (1979).

19) A. M. Bradshaw and F. M. Hoffmann, Surface Sci. 72, 513 (1978).

20) T. E. Madey, J. E. Houston and S. C. Dahlberg, in D. A. Degras and M. Costa, eds. Proceedings of the 4th International Conference on Solid Surfaces and the 3rd European Conference on Surface Science, Cannes, France (Supplement a la Revue "Le Vide, les Couches Minces" no. 201) p. 205.

21) N. V. Richardson and A. M. Bradshaw, Surface Science 88, 255 (1979).

22) T. E. Madey, Surface Science 94, 483 (1980).

23) K. Besocke and S. Berger, in: Proc. 7th Intern. Vac. Congr. and 3rd Intern. Conf. on Solid Surfaces, Vienna, 1977, Eds. R. Dobrozemsky et. al. (Berger, Vienna, 1977) p. 893.

24) R. Gomer, Japan J. Appl. Phys., Suppl. 2, Pt. 2, 213 (1974); Ch. Steinbruchel and R. Gomer, Surface Science 67, 21 (1977).

25) E. W. Plummer, B. J. Waclawski, T. V. Vorburger and C. E. Kuyatt, Prog. in Surface Sci. 7, 149 (1976).

26) R. Jaeger and D. Menzel, Surface Sci. 93, 71 (1980).

27) See, for example, (a) V. N. Ageev and N. I. Ionov in: Progress in Surface Sci. Vol. 5, Ed. S. G. Davison (Pergamon, New York, 1975) p. 1, (b) T. E. Madey, Surface Sci. 33, 355 (1972), (c) D. A. King, T. E. Madey and J. T. Yates, Jr., J. Chem. Soc., Faraday Transactions I, 68, 1347 (1972).

28) B. Krahl-Urban and H. Niehus, Surface Science 88, L19 (1979).

29) M. A. van Hove and S. Y. Tong, Phys. Rev. Letters 35, 1092 (1975).

30) T. E. Madey and J. T. Yates, Jr. in: Proc. 7th Intern. Vac. Congr. and 3rd Intern. Conf. on Solid Surfaces, Berger, Vienna, 1977) p. 1183.

31) T. E. Madey, J. E. Houston, C. Seabury and T. N. Rhodin, J. Vac. Sci. Technol., to be published.

32) P. A. Thiel, F. M. Hoffmann and W. H. Weinberg, in D. A. Degras, Proceedings of the 4th International Conference on Solid Surfaces and the 3rd European Conference on Surface Science, Cannes, France (Supplement a la Revue "Le Vide, les Couches Minces" no. 201) p. 307.

33) J. Gersten, R. Janow and N. Tzoar, Phys. Rev. Lett. 36, 610 (1976).

34) W. L. Clinton, Phys. Rev. Lett. 39, 965 (1977). W. L. Clinton, to be published.

35) a) J. W. Gadzuk, Surface Sci. 67, 77 (1977).
b) J. W. Gadzuk, Phys. Rev. B14, 2267 (1976).

36) D. Lichtman and Y. Shapira, Crit. Rev. Solid State Sci. 7, 167 (1978).

37. J. F. van der Veen, F. J. Himpsel, D. E. Eastman and P. Heimann, Solid State Communications, 36, 99 (1980).

38) D. E. Eastman, J. J. Donelon, N. C. Hien and F. J. Himpsel, J. Nucl. Inst. Methods, 172, 327 (1980).

39) L. Fiermans and J. Vennik, Surf. Sci. 9, 187 (1968).

40) T. E. Madey, J. J. Czyzewski and J. T. Yates, Jr., Surface Sci. 57, 580 (1976).

41) H. Niehus, Surf. Sci., 87, 561 (1979).

42) Photoemission in Solids I, M. Cardona and M. Loy, eds., in Topics in Applied Physics, Vol. 26 (Springer-Verlag, New York 1978).

43) R. Jaeger, J. Feldhaus, J. Haase, J. Stohr, Z. Hussain, D. Menzel, and D. Norman, Phys. Rev. Lett. 45, 1870 (1980).

44) T. A. Carlson and M. O. Krause, J. Chem. Phys. 56, 3206 (1972).

45) J. E. Houston and T. E. Madey, to be published.

46) R. Treichler and D. Menzel, to be published.

47) D. Jennison and J. Kelber, to be published.

48) D. A. Ramaker, C. T. White and J. Murday, to be published.

49) D. Menzel, in D. A. Degras and M. Costa, eds. Proceedings of the 4th International Conference on Solid Surfaces and the 3rd European Conference on Surface Science, Cannes, France (Supplement a la Revue "Le Vide, les Couches Minces" no. 201) p. 1259.

50) T. E. Madey, R. Stockbauer, S. A. Flodstrom, J. F. van der Veen, F. J. Himpsel and D. E. Eastman, to be published.